Structures and Magnetic Properties of [*o*- and *p*-MePyNN$^+$]$_2$[Cu(ox)$_2$] (MePyNN$^+$ = Nitronyl Nitroxyl Radical Cation)

Hiroki Oshio,* Taira Yaginuma, and Tasuku Ito

Department of Chemistry, Graduate School of Science, Tohoku University, Aoba-ku, Sendai 980-8578

(Received December 7, 1999)

Reactions of [*o*-MePyNN$^+$]PF$_6$ and [*p*-MePyNN$^+$]PF$_6$ with [*n*-Bu$_4$N]$_2$[Cu(ox)$_2$] in acetonitrile yielded dark-blue crystals of [*o*-MePyNN$^+$]$_2$[Cu(ox)$_2$]·2CH$_3$OH (**1**) and [*p*-MePyNN$^+$]$_2$[Cu(ox)$_2$]·2H$_2$O (**2**), respectively, where [*o*-MePyNN$^+$] or [*p*-MePyNN$^+$] represents the 2-(2 or 4-*N*-methylpyridinium)-4,4,5,5-tetramethyl-4,5-dihydro-1*H*-imidazo-1-oxyl 3-oxide radical cation. X-ray structural analyses showed that the crystals of **1** and **2** are isomorphous. The coordination geometry of the Cu^{2+} ions in **1** and **2** is an elongated octahedron, and the equatorial and apical coordination sites of the Cu^{2+} ions are occupied by two oxalato groups and two radial cations, respectively. Magnetic susceptibility measurements for **1** and **2** revealed that the copper and radical centers are ferromagnetically coupled with J = +8.2(1) and +7.8(1) cm^{-1} ($H = -2J\sum S_{Cu}\cdot S_{rad}$), respectively.

There has been increasing interest in molecule based magnetic materials. Since the discovery of ferrimagnetic ordering in [Mn(hfac)$_2$][NITR] (hfac = hexafluoroacetylacetone and NITR = 2-isoproyl-4,4,5,5-tetramethyl-4,5-dihydro-1*H*-imidazo-1-oxyl 3- oxide),[1] nitronyl niroxyl derivatives have been widely used as building components of magnetic materials. It is noted that inter molecular magnetic interactions are indispensable to bulk magnetism. In ionic compounds, for example, diamagnetic counter ions might interfere such intermolecular, interchain, or inter-layer magnetic interactions. This situation is considered to be disadvantageous for bulk magnetism. The introduction of ionic radicals to metal complexes gives, therefore, an opportunity to extend the dimension of magnetic interactions. An anionic radical ligand of a nitronyl nitroxyl derivative with imidazolate fragment ([NITIm]$^-$) has been reported to act as a bischelating ligand, and the one-dimensional structure of [Mn(NITIm)(NITImH)]ClO$_4$ was obtained (NITIm = 2-(2-imidazolato)-4,4,5,5-tetramethyl-4,5-dihydro-1*H*-imidazolyl-3-oxide-1-oxyl and NITImH = 2-(2-imidazolyl)- 4,4,5,5-tetramethyl-4, 5- dihydro- 1*H*- imidazolyl- 3- oxide- 1- oxyl).[2] Radical cations of *N*-methylpyridinium nitronyl nitroxide (MePyNN$^+$) were, on the other hand, prepared by K. Awaga.[3] In the crystals of [*p*-MePyNN](ClO$_4$) and [*p*-MePyNN]I, the radical cations have dimeric structures with a short intermolecular NO contact (3.159(8) Å), which resulted in relatively strong intra-dimer antiferromagnetic interactions with singlet-triplet energy gaps of 100 cm^{-1}. O. Kahn et al. reported open-shell supramolecular assemblies of radical cationic salts with [Fe(CN)$_6$]$^{3-}$ and Mn$_2$[Cu(opba)]$_3^{2-}$ (opba = *o*-phenylenebis(oxamato)) which showed three dimensional magnetic interactions.[4,5] Here, we report a new series of metal complexes with radical cations, [*o*-MePyNN$^+$]$_2$[Cu(ox)$_2$]·2CH$_3$OH (**1**) and [*p*-MePyNN$^+$]$_2$[Cu(ox)$_2$]·2H$_2$O (**2**), of which structure and magnetic properties are presented.

Experimental

Chemicals were obtained from standard sources and were used as received. Magnetic susceptibility data were collected in the temperature range of 2.0 to 300 K and in an applied 10 kG field with the use of a Quantum Design model MPMS SQUID magnetometer. Pascal's constants[6] were used to determine the constituent atom diamagnetism.

Preparation of [*o*-MePyNN$^+$]$_2$[Cu(ox)$_2$]·2CH$_3$OH (1) and [*p*-MePyNN$^+$]$_2$[Cu(ox)$_2$]·2H$_2$O (2).[7] Acetonitrile solutions (20 ml) of [*o*-MePyNN](PF$_6$) (79 mg, 0.20 mmol) and [*o*-MePyNN](PF$_6$) (79 mg, 0.20 mmol), were, respectively, added to [*n*-Bu$_4$N]$_2$[Cu(ox)$_2$][8] (73 mg, 1 mmol) in acetonitrile (20 ml). After stirring for 1 h, the insoluble solids were filtered out, and the filtrate was stored in a refrigerator. After standing overnight the resulting dark green tablets of **1** and **2** were filtered and washed with methanol. (Found for **1**: C, 48.50; H, 5.36; N, 11.09%. Calcd for C$_{30}$H$_{12}$CuN$_6$O$_{12}$: C, 48.81; H, 5.19; N, 11.38%, and Found for **2**: C, 46.32; H, 5.29; N, 11.04%. Calcd for C$_{30}$H$_{16}$CuN$_6$O$_{14}$: C, 46.54; H, 5.47; N, 10.85%.

X-Ray Crystallography. A single crystal was mounted on the tips of glass fiber with epoxy resin. Diffraction data were collected at −70 °C on a Bruker SMART 1000 diffractometer fitted with a CCD-type area detector, and a full sphere of data was collected by using graphite-monochromated Mo $K\alpha$ radiation (λ = 0.71073 Å). At the end of the data collection, the first 50 frames of data were recollected to establish that crystal decay had not taken place during the data collection. The data frames were integrated using SAINT, and were merged to give a unique data set for the structure determination. Empirical absorption corrections by SADABS were carried out and minimum–maximum transmissions for **1** and **2** were 0.830—1.000 and 0.876—0.998, respectively. The crystallographic data are listed in Table 1. The structures were solved by the direct method and refined by the full-matrix least-squares method on all F^2 data using the SHELXTL 5.1 package (Bruker Analytical X-ray Systems). Non-hydrogen atoms were refined with anisotropic thermal parameters. Hydrogen atoms were included in

Table 1. Crystal Data and Structure Refinements for [*o*-MePyNN$^+$]$_2$[Cu(ox)$_2$]·2CH$_3$OH (**1**) and [*p*-MePyNN$^+$]$_2$[Cu(ox)$_2$]·2H$_2$O (**2**)

Compounds	**1**	**2**
Formula	$C_{32}H_{46}CuN_6O_{14}$	$C_{30}H_{42}CuN_6O_{14}$
M	802.30	774.25
Temperature/°C	−70	−70
Crystal system	Triclinic	Triclinic
Space group	$P\bar{1}$	$P\bar{1}$
a/Å	8.0738(3)	7.1493(6)
b/Å	10.8087(4)	10.3889(9)
c/Å	10.9839(5)	11.7450(10)
α/°	102.7840(10)	104.443(2)
β/°	103.1840(10)	97.822(2)
γ/°	96.4420(10)	97.558(2)
U/Å^3	896.68(6)	824.37(12)
Z	1	1
D_c/g cm^{-3}	1.427	1.524
μ/mm^{-1}	0.607	0.606
Crystal size/mm^3	0.2 × 0.3 × 0.3	0.2 × 0.3 × 0.3
Reflections collected	4377	4324
Independent reflections	3437 [*R*(int) = 0.0275]	3628 [*R*(int) = 0.0348]
Final *R* indices [$I > 2\text{sigma}(I)$]	*R*1 = 0.0482, *wR*2 = 0.1342	*R*1 = 0.0526, *wR*2 = 0.1512
R indices (all data)	*R*1 = 0.0580, *wR*2 = 0.1406	*R*1 = 0.0669, *wR*2 = 0.1692

$R1 = \sum||F_o| - |F_c||/\sum|F_o|$.
$wR2 = [\sum[w(F_o^2 - F_c^2)^2]/\sum[w(F_o^2)^2]]^{0.5}$,
calc $w = 1/[\sigma^2(F_o^2) + (0.0992P)^2 + 0.1763P]$ for (**1**),
and $w = 1/[\sigma^2(F_o^2) + (0.1154P)^2 + 0.000P]$ for (**2**), where $P = (F_o^2 + 2F_c^2)/3$.

the calculated positions and refined with isotropic thermal parameters riding on those of the parent atoms. The X-ray analyses data have been deposited as Document No.73033 at the Office of the Editor of Bull. Chem. Soc. Jpn. Crystallographic data have been also deposited at the CCDC, 12 Union Road, Cambridge CB2 1EZ, UK and copies can be obtained on request, free of charge, by quoting the publication citation and the deposition CCDC 141929-141930.

Results and Discussion

Structures. Complexes of [*o*-MePyNN$^+$]$_2$[Cu(ox)$_2$]·2CH$_3$OH (**1**) and [*p*-MePyNN$^+$]$_2$[Cu(ox)$_2$]·2H$_2$O (**2**) crystallize in the triclinic space group of $P\bar{1}$. Figure 1 shows ORTEP diagrams of **1** and **2**, and Table 2 lists the selected bond lengths and angles. The crystals of **1** and **2** are isomorphous and the complex molecules locate on the crystallographic center of symmetry. The coordination geometry about the Cu^{2+} ions can be described by the elongated octahedron, which is due to the Jahn–Teller distortion of the Cu^{2+} ions. The equatorial coordination sites of the Cu^{2+} ion were occupied by four oxygen atoms from two oxalato ligands, while two oxygen atoms of the radical cations (*o*-MePyNN$^+$ or *p*-MePyNN$^+$) coordinated to the Cu^{2+} ions from the apical positions. In **1** and **2**, the bond lengths of the Cu^{2+} ions with oxalato oxygen atoms are in the range of 1.929(2)—1.938(2) Å, where the other oxalato oxygen atoms do not have close contacts with atoms in the next molecule. The Cu^{2+}–O(nitroxide) bond distances for **1** and **2** are 2.607(2) and 2.801(2) Å, respectively, and the axial bonds of Cu^{2+}–O(nitroxide) are titled by 6.48(7)° for **1** and 14.67(7)° for **2** with respect to the right angle of the equatorial plane.

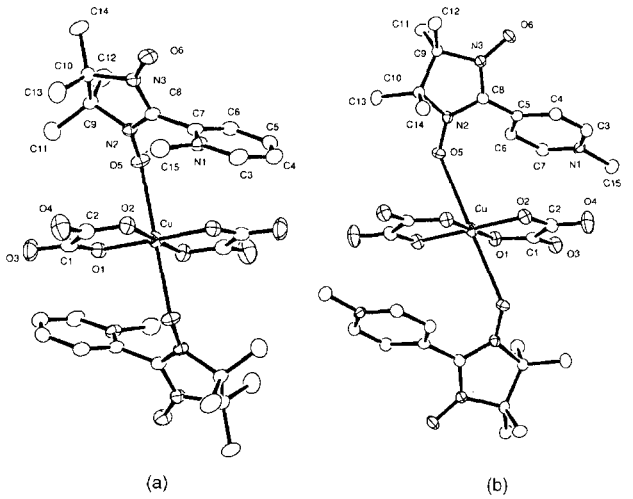

Fig. 1. Ortep diagrams of (a) [*o*-MePyNN$^+$]$_2$[Cu(ox)$_2$] (**1**) and (b) [*p*-MePyNN$^+$]$_2$[Cu(ox)$_2$] (**2**).

Magnetic Properties. The temperature dependences of the magnetic susceptibility for **1** and **2** were measured down to 2.0 K, and plots of $\chi_m T$ vs. temperature are depicted together in Fig. 2. In **1** and **2**, the Cu^{2+} ions are coordinated by two of the racial cations; therefore, each complex molecule has three of $S = 1/2$ spins. The room temperature $\chi_m T$ values for **1** and **2** are about 1.18 emu^{-1} K mol^{-1}, which corresponds to the value for the uncorrelated three spin system. The $\chi_m T$ values for **1** monotonously increased as the temperature was lowered to 2.0 K, while the $\chi_m T$ value for **2** showed

Table 2. Bond Lengths [Å] and Angles [°] for [*o*-MePyNN$^+$]$_2$[Cu(ox)$_2$]·2CH$_3$OH (**1**) and [*p*-MePyNN$^+$]$_2$[Cu(ox)$_2$]·2H$_2$O (**2**)

	1	**2**
Cu–O(1)	1.934(2)	1.938(2)
Cu–O(2)	1.932(2)	1.929(2)
Cu–O(5)	2.607(2)	2.801(2)
O(1)–C(1)	1.278(4)	1.291(4)
O(2)–C(2)	1.286(3)	1.284(4)
O(3)–C(1)	1.229(4)	1.223(4)
O(4)–C(2)	1.226(4)	1.218(4)
O(5)–N(2)	1.277(3)	1.283(3)
O(6)–N(3)	1.272(3)	1.275(3)
O(2)–Cu–O(1)	85.67(8)	85.36(8)
O(2)–Cu–O(5)	86.33(7)	77.70(8)
O(1)–Cu–O(5)	84.40(7)	98.84(8)

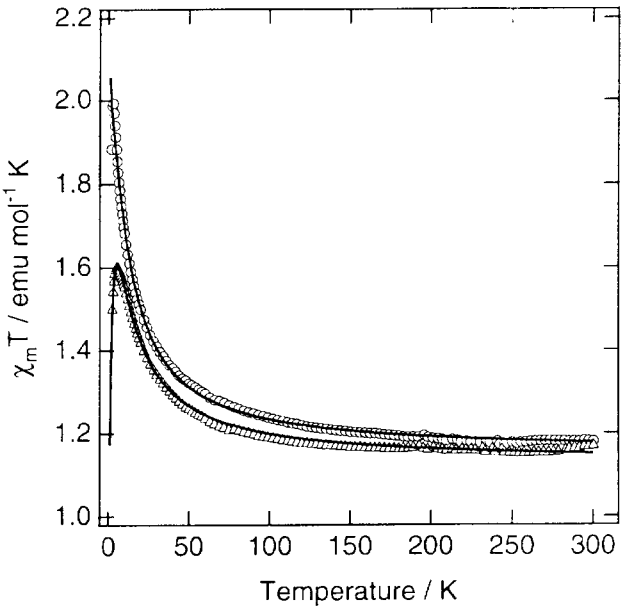

Fig. 2. $\chi_m T$ vs. T plot for **1** (○) and **2** (△). Solid lines correspond to the theoretical curves, of which parameters are given in the text.

a gradual increase as the temperature was lowered, reaching the maximum value (1.60 emu^{-1} K mol^{-1}) at 6.0 K, and then decreased. The observed magnetic behaviour suggests that intramolecular ferromagnetic interactions are operative for **1** and **2**, and that relatively weak inter-molecular antiferromagnetic interaction exists in **2**. The magnetic data for **1** and **2** were analyzed by the linear three spin system of $S = 1/2$ with an isotropic spin hamiltonian of $H = -2J\sum S_{Cu}\cdot S_{rad}$, where J represents the magnetic interaction between the Cu^{2+} ion and the radical cations. Intermolecular interactions are included as a mean field correction. The expression for χ_m is as follows:

$$\chi_m = \frac{Ng^2\beta^2}{4k(T-\theta)}\frac{1+\exp(-2J/kT)+5\exp(J/kT)}{1+\exp(-2J/kT)+2\exp(J/kT)}.$$

Least squares calculations yielded the best fit parameters of the g, J, and θ values, being 2.020(1), +8.2(1) cm^{-1}, and −0.01(1) K for **1** and the corresponding values of 2.000(1), 7.8(1) cm^{-1}, and −0.6(1) K were obtained for **2**. The magnetic interaction between the Cu^{2+} ions with the coordinated nitoxides depends on which coordination sites nitroxides take. The equatorial coordination of the nitroxides often results in a strong antiferromagnetic interaction due to the substantial overlap of the nitroxide SOMO with the $d_{x^2-y^2}$ orbital.[9] On the other hand, a relatively strong ferromagnetic interaction ($J = -25.7$ cm^{-1} with $H = \sum J_{ij}S_i\cdot S_j$) between the Cu^{2+} ion and nitroxides was observed in *catena*-[Cu(hfac)$_2$(NIT–Me)] (NIT–Me = 2,4,4,5,5-pentamethyl-1-oximidazoline-3-oxide), where the nitroxides coordinate to the Cu^{2+} ion from the axial position.[10] The weaker ferromagnetic interaction observed in **1** and **2** can be understood by the more elongated Jahn–Teller distortion in **1** and **2**; that is, the Cu^{2+}–O(nitroxide) bond distances for **1** and **2** are 2.607(2) and 2.801(2) Å, while the corresponding bond distances in *catena*-[Cu(hfac)$_2$(NIT–Me)] were reported to be 2.346(8) and 2.433(7) Å.

X-ray structure analyses for **1** and **2** revealed that the equatorial coordination bond lengths are much shorter than the axial coordination bond lengths; this means that the unpaired electron (σ-spin) of the Cu^{2+} ion resides on the $d_{x^2-y^2}$ orbital. Because the two radical cations (π-spin) coordinate from the axial position of the Cu^{2+} ions, the overlap of the $d_{x^2-y^2}$ orbital of the Cu^{2+} ion with the SOMO (singly occupied molecular orbital) of the radical cations is considered to be very small, which results in intramolecular ferromagnetic interactions in **1** and **2**. The observed weak inter-molecular antiferromagnetic interactions can be understood by the close contact of the nitroxyl (N–O) with the pyridinum group in the adjacent molecule. In nitronyl nitroxyl derivatives, the radical π-spin delocalizes mainly onto the nitroxide groups, and a small portion of spin also delocalizes onto an aromatic group bonded to the sp^2 carbon atom bridging the two N–O groups and positive and negative spins are alternately aligned in the pyridinium group (Fig. 3).[11] In the crystal of **2**, the N–O group has the closest contact (3.108(3) Å) with the pyridinium C3 atom of the next molecule, of which the contact mode stabilises the anti-parallel spin alignment in the stacked molecules due to the McConnell mechanism.[12] On the other hand, the corresponding inter atomic contact (3.597(3) Å) in **1** is longer than **2**, which results in the negli-

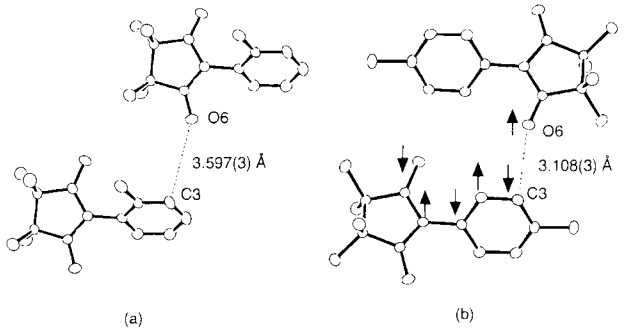

Fig. 3. Radical stacking diagrams in (a) **1** and (b) **2**.

gibly weak inter-molecular antiferromagnetic interactions in **1**.

This work was partially supported by a Grant-in-Aid for Scientific Research from the Ministry of Education, Science, Sports and Culture.

References

1 A. Caneschi, D. Gatteschi, J. P. Renard, P. Ray, and R. Sessoli, *Inorg. Chem.*, **28**, 1976 (1989); A. Caneschi, D. Gatteschi, P. Ray, and R. Sessoli, *Acc. Chem. Res.*, **22**, 392 (1989).

2 K. Fegy, D. Luneau, E. Belorizky, M. Novac, J-L. Tholence, C. Paulsen, T. Ohm, and P. Ray, *Inorg. Chem.*, **37**, 4524 (1998).

3 A. Yamaguchi, K. Awaga, T. Inabe, T. Nakamura, M. Matsumoto, and Y. Maruyama, *Chem. Lett.*, **1991**, 1777; A. Yamaguchi, K. Awaga, T. Inabe, T. Nakamura, M. Matsumoto, and Y. Maruyama, *Chem. Lett.*, **1993**, 143.

4 C. Micahut, L. Ouahab, P.Bergerat, O. Kahn, and A. Bousseksou, *J. Am. Chem. Soc.*, **118**, 3610 (1996).

5 H. O. Stumph, L. Ouahab, Y. Pei, D. Grandjean, and O. Kahn, *Science*, **261**, 447 (1993); H. O. Stumph, L. Ouahab, Y. Pei, P. Bergerat, and O. Kahn, *J. Am. Chem. Soc.*, **116**, 3386 (1994).

6 W. E. Hatfield, "Theory and Application of Molecular Paramagnetism," ed by E. A. Boudreaux and L. N. Mulay, Wiley and Sons, Inc., New York (1976), p. 491.

7 We tried to prepare a complex of $[m\text{-MePyNN}^+]_2[\text{Cu(ox)}_2]$, however, we could not obtained the fine single crystal suitable for the X-ray analysis.

8 X. Wang, C. Ge, X. Xing, P. Wang, D. Zhnf, P. Wu, and D. Zhu, *Synth. Met.*, **39**, 355 (1991).

9 J. Laugier, P. Rey, C. Benelli, D. Gatteschi, and C. Zanchini, *J. Am. Chem. Soc.*, **108**, 6931 (1986).

10 A. Caneschi, D. Gatteschi, J. Laugier, and P. Rey, *J. Am. Chem. Soc.*, **109**, 2191 (1987).

11 K. Yamaguchi, M. Okumura, and M. Nakano, *Chem. Phys. Lett.*, **191**, 237 (1992).

12 H. M. McConnell, *J. Chem. Phys.*, **39**, 1910 (1963).